HAL
open science

# All-printed infrared sensor based on multiwalled carbon nanotubes

Aurelien Gohier, Anirban Dhar, Louis Gorintin, Paolo Bondavalli, Yvan Bonnassieux, Costel Sorin Cojocaru

## To cite this version:

Aurelien Gohier, Anirban Dhar, Louis Gorintin, Paolo Bondavalli, Yvan Bonnassieux, et al.. All-printed infrared sensor based on multiwalled carbon nanotubes. Applied Physics Letters, 2011, 98, pp.063103. 10.1063/1.3552686 . hal-00794034

**HAL Id: hal-00794034**

**https://hal.science/hal-00794034v1**

Submitted on 2 Mar 2013

**HAL** is a multi-disciplinary open access archive for the deposit and dissemination of scientific research documents, whether they are published or not. The documents may come from teaching and research institutions in France or abroad, or from public or private research centers.

L'archive ouverte pluridisciplinaire **HAL**, est destinée au dépôt et à la diffusion de documents scientifiques de niveau recherche, publiés ou non, émanant des établissements d'enseignement et de recherche français ou étrangers, des laboratoires publics ou privés.

# APPLIED PHYSICS LETTERS

***98**, 063103 (2011)*
*doi:10.1063/1.3552686*


## All-printed infrared sensor based on multiwalled carbon nanotubes


**A. Gohier,[1] A. Dhar,[1] L. Gorintin,[2] P. Bondavalli,[2] Y. Bonnassieux,[1] and C. S. Cojocaru[1,a)]**

[1]*Laboratoire de Physique des Interfaces et des Couches Minces, Ecole Polytechnique, UMR7647CNRS, route de Saclay, 91128 Palaiseau Cedex, France*

[2]*Thales Research and Technology France, D128 91767 Palaiseau Cedex, France*



ABSTRACT

This contribution deals with all-printed infrared sensors fabricated using multiwalled carbon nanotubes deposited on a flexible polyimide substrate. A high responsivity of up to 1.2 kV/W is achieved at room temperature in ambient air. We evidence a strong dependence of the device transduction mechanism on the surrounding atmosphere, which can be attributed to bolometric effect interference with water molecule desorption upon irradiation.


Random carbon nanotube (CNT) networks advantageously combine the ease of integration and processing proper to organic materials and the possibility of exploiting some interesting physical properties proper to inorganic materials. Such unconventional features motivate the increasing CNT mats interest for many electronic applications such as electrodes,[1] transistors,[2] and sensors.[3] Among CNTs based sensors, photosensors and especially infrared (IR) sensors[4–8] have recently attracted much attention, since CNTs exhibit wide absorbance in the infrared range.[9] Despite numerous works devoted to CNTs based photo- sensors, the origin of the large photoresponse is still subject to considerable debate. Two main mechanisms have been proposed to explain the photosignal in CNT films: (i) Bolometric effect (change of resistance due to heating)[5,8,10,11] and (ii) free charge carrier generation.[6,7,12] While bolometric effect has been clearly pointed out on suspended (free- standing) CNT mat by Itkis *et al.*,[5] the generation of free carrier has been also demonstrated, especially at the metal CNT interface where excitons can be separated more easily.[6] These two mechanisms may both occur with a magnitude depending on the specific CNT mats composition (single- walled nanotubes, multiwalled nanotubes, nanotubes/ polymer composite, etc.), CNT mats morphology (unsuspended/suspended CNT film), and also on the laser illumination position. Hence, the optimization of CNTs based photosensors response often requires specific improvement related to the main transduction mechanism involved in the device. More specifically, for CNTs based bolometers, it is well known that suspended CNTs can lead to a significant enhancement of the responsivity.[11] Using thermally insulating substrate such as plastic materials can offer an attractive al- ternative approach to limit thermal leakage between the sen- sitive element and the substrate.[13] Moreover, flexible plastic substrate also offers opportunities for bolometer integration into brand new areas, such as smart skins or wearable body monitoring systems. In this letter, we present the realization of an all-printed CNTs based IR sensor on polyimide flexible substrates. Taking advantage of the printability of CNT aqueous dispersions, we have studied the ink-jet printing process as a means of low cost IR sensor integration with high scalability potentialities. Flexible capton(™) polyimide sheets with a thickness of 110 μm were used as substrate (Fig. 1(a)). The electrodes were printed with highly conductive silver ink ($\sigma \sim 0.625 \times 10^6$ S / cm) from InkTek Corp, Korea, using a Dimatix Material Printer (DMP-2800 by FUJIFILM, USA). At first, a resistance is plotted as a function of time during device exposure to intermittent near infrared (NIR) irradiation. The device was biased at 0.2 V and the NIR laser beam (0.5 $mW.mm^{-2}$) was delivered by an 850 nm laser diode controlled with a Thorlabs LDC205C apparatus. The laser power density was calibrated using a thermal power meter (Thorlabs S210A).The response to the incident light is clearly identified as a significant resistance drop of ~0.35%, which could be observed after 10 s of illumination. The initial resistance can then be fully recovered when the laser is turned off after

the same time period (Fig. 2(a)). As shown in Fig. 2(b), the amplitude of the response linearly depends on the incident light power (Fig. 2(b)).

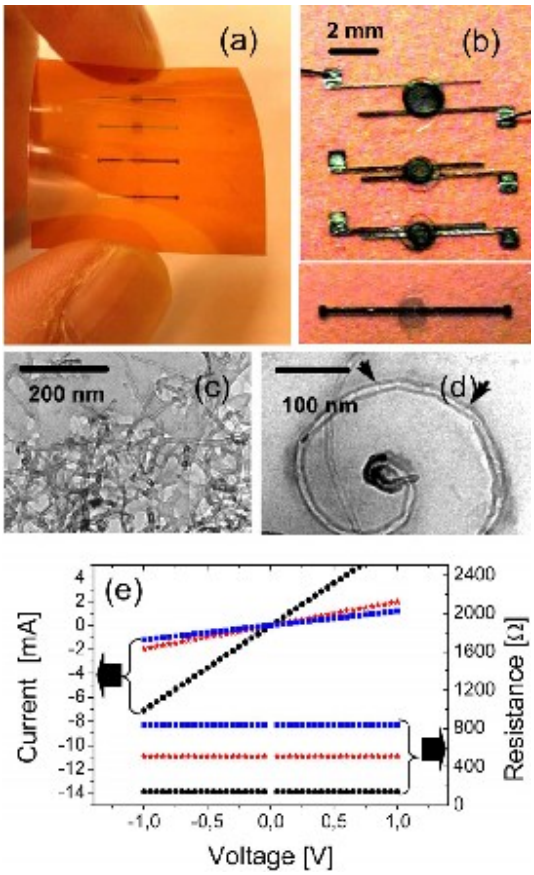


FIG. 1. (Color online) (a) Set of printed samples on flexible polyimide substrate. (b) Optical image of the devices. (c) Low magnification TEM picture of the MWCNTs. (d) High magnification TEM picture of the MWCNTs. The arrows indicate "bamboo-type" defects in the nanotubes structure. (e) I-V curves of devices as a function of the channel length (dots:

The performance of the photo sensor can be expressed in terms of responsivity $R_v$, which is defined as a change of output voltage for a change of incident power ($\Delta V / \Delta P$). In the particular case of bolometers, $R_v$ can be expressed as $(RI\alpha\eta) / (G^2 + \omega^2 C^2)^{1/2}$, where $R$ is the device resistance, $I$ is the forcing current, $\alpha$ is the temperature coefficient of resistance, $\eta$ is the optical absorption coefficient, $G$ is the thermal conductance to the heat sink, $C$ is the heat capacity of the sensitive element, and $\omega$ is the modulation frequency. Figure 2(c) plots the responsivity as a function of the design consisting of a set of parallel electrodes with various channel lengths from 50 to 1100 J..m was printed (Fig. 1(b), upper panel). Another design that enables a smaller sensitive area (200 X 50 J..m) was also realized (Fig. 1(b), lower panel). Multiwalled (MW) carbon nanotubes (CVD-grown, from Arkema Corporation) were used as sensitive material. They have typical diameters in the range of 10–20 nm with a length between 1 and 10 J..m (Fig. 1(c)). TEM investigations (Philips CM 30 working at 300 kV) revealed many structural defects such as inner compartments (Fig. 1(d), arrows) indi- cating a nanotube morphology closer to bamboo-like type. MWCNT dispersion was prepared in water/1-propanol mixture (4 : 1 wt. %) using sonication probe and nafion as surfactant (1 wt. %). The CNT suspension was then centrifuged and the supernatant was removed to keep the stable part of the dispersion. MWCNTs were then precisely deposited in a channel region between the silver printed electrode by a Drop-On-Demand printer (Ultra TT series, EFD). Several prints were necessary to achieve a percolated network of MWCNTs in the active region of the device. Electrical measurements were carried out using a Kei- thley 4200 semiconductor characterization unit. The current- voltage recordings are displayed in Fig. 1(e). For every de- vice, a linear trend is observed, emphasizing the ohmic behavior of the MWCNT network. As expected, the resistance of the

device resistance strongly depends on the elec- trode geometry (for a given amount of CNTs) and becomes larger as the channel length is increasing (from 140 to 850 Ω).

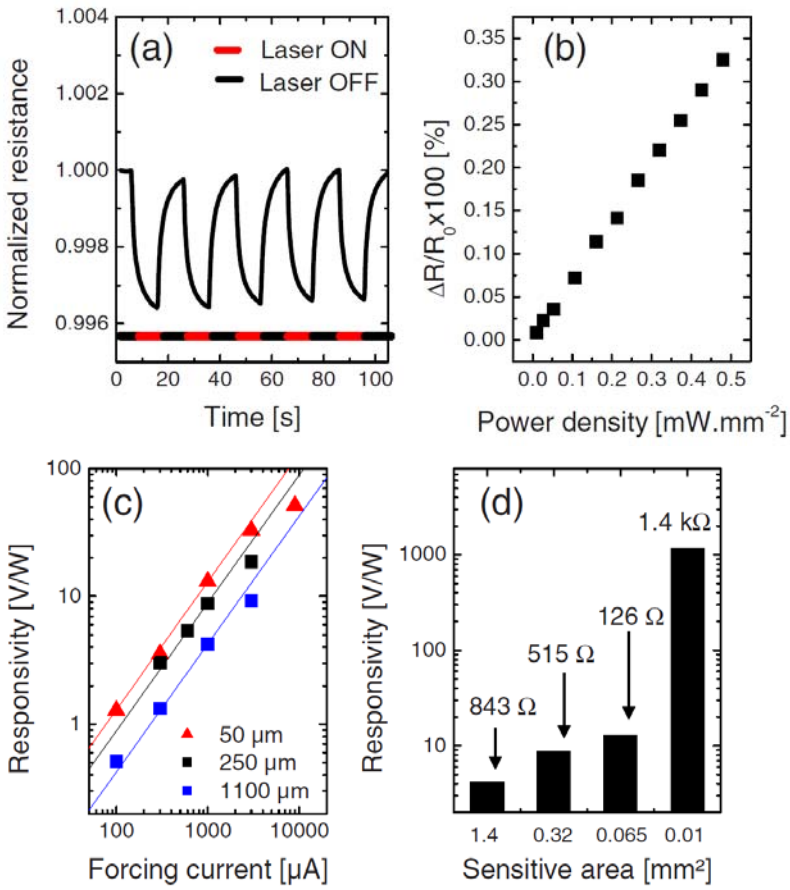


FIG. 2. (Color online) (a) Photoresponse of the device with 1100 J..m channel length biased at 0.2 V. IR power is ~0.5 mW · mm$^{-2}$. (b) Photoresponse as a function of the power density of the incident radiation. (c) Responsivity of three devices as a function of the channel length and the forcing current. (d) Responsivity for a forcing current 1 mA as a function of the sensitive area and the resistance.

Figure 2(a) displays a typical photoresponse measured for the device with the larger channel gap. The electrical forcing current (from 100 J..A to 9 mA) for three devices with various channel gaps. All devices show the same linear trend as a function of the forcing current. Obviously, for a given resistance of the device, the higher is the forcing cur- rent, the higher is the responsivity. In fact, the maximum current is limited by the heat produced under current flow ($RI^2$). At high values, this can damage the nanotube network and, in our case, can melt the substrate. As a result, the maximum current we imposed was 10 mA for a 140 Ω resistance device. For constant forcing current value, the sensitive area is shown to strongly impact the responsivity. The higher re- sponsivity is observed for the smaller channel gap despite lower values of electrical resistance (Fig. 2(d)). Taking into account these observations, we optimized the sensor design to obtain a small sensitive area of ~$10^4$µm$^2$ that can with- stand 1 mA current through a resistance of 1.4 kΩ. With these features, a responsivity of ~1160 V / W can be obtained (Fig. 2(d)). This is more than four times higher than the recent maximum report ~250 V / W that used suspended single-walled carbon nanotubes as sensitive element.[11] Such size effect could be related to the expression of $R_v$, since $C$ as well as $G$ are extensive values that depend on the size of the sample. To verify such an assumption, we further focused on the transduction mechanism involved in the sens- ing. As shown in Fig. 3(a), the device exhibits a negative temperature coefficient of resistance (TCR) of ~0.19% K$^{-1}$. This last is comparable with previous reports on multi-walled carbon nanotubes[14–16] as well as single-walled nanotubes[5,17–19] and is consistent with bolometric behavior as the resistance drops when illuminating the MWCNT net- work. Along with the temperature variation, we also

stressed out a strong correlation between the device resistance and the surrounding relative humidity (measured by the multifunc- tional transmitter of EE31-E series produced by E + E manu- facturer). As shown in Fig. 3(b), the resistance significantly drops when decreasing the humidity amount. The sign of this chemical response underlines that water molecule desorption

The response time ($R / R_0 = 0.63R_{max} / R_0$) is around ~1 s, independently on the device surrounding atmosphere (Fig. 4). This quite large response time has already been observed in the case of unsuspended CNTs[4,11,22] films as well as suspended ones.[8] As the response time ,. scales as $C / G$ in the case of bolometers, the response time may be further improved by optimizing these two parameters. For instance, using better crystalline quality and longer carbon nanotubes could decrease the heat capacity of the CNT network while decreasing its thermal conductance. In conclusion, we developed an all-printed NIR sensor on flexible substrate based on multiwalled carbon nanotubes could be triggered under the laser irradiation, leading to enhanced photoresponse.[20] In order to discriminate the relative humidity effect from the bolometric effect, the photoresponse was plotted as a function of different surrounding atmosphere (Fig. 4). When the amount of relative humidity is decreased from 55% in air (black line) to 0.6% (light grey line), the photoresponse is subsequently reduced by ~80% ($\Delta R / R_0 = 0.07\%$ instead of 0.37%). The result points out the importance of the humidity in the sensing mechanism. It could be attributed to the nafion polymer, used here as surfactant, which has already shown its ability to greatly adsorb water molecules via its hydrophilic sulfonated groups.[21] Interestingly, for the same low level of relative humidity (0.6%), the photoresponse is enhanced by a factor 3.3 when the device is put in vacuum ($\Delta R / R_0 = 0.23\%$ instead of 0.07%, grey line). This increase is attributed to an enhance- ment of the expected bolometric effect as the thermal link is reduced in vacuum. Hence, while water molecule desorption triggers the photosignal in wet atmosphere, the bolometric effect becomes predominant in vacuum. Note that the side effect induced by water molecules could be suppressed whether by passivating the CNT network and we are currently working on this improvement.

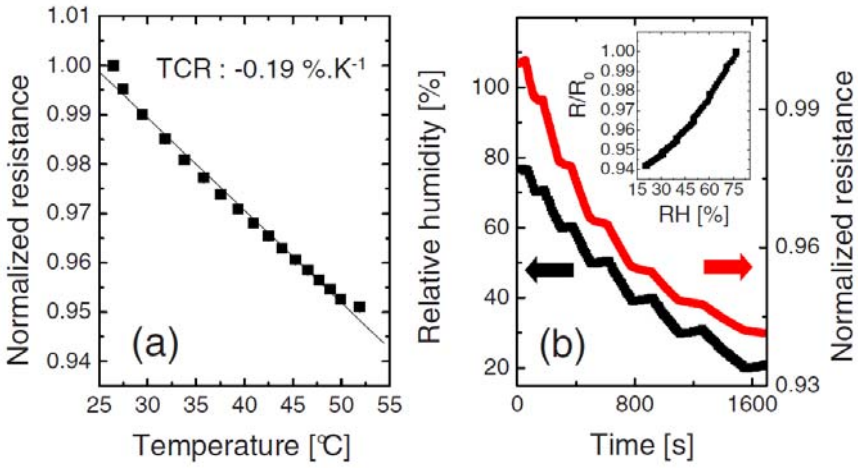


FIG. 3. (Color online) (a) Device resistance as a function of the temperature range of 25 – 50 ° C. (b) Resistance evolution as a function of the amount of humidity. The arrow indicates a weak variation of humidity.

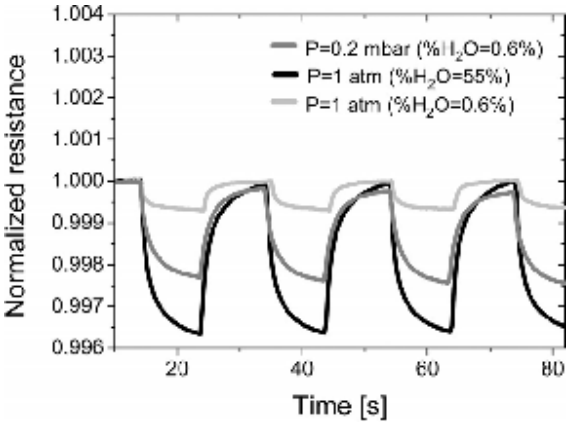


FIG. 4. Device photoresponse as a function of the atmosphere.

This approach enables the development of a low-cost fully integrated CNT based IR sensor array with responsivity up to 1.2 kV/W. In addition to the primary bolometric effect, we highlighted the role played by relative humidity in the photosignal generation when such devices operate in ambient air. Further improvement of the MWCNT network morphology will be devoted to limit this side effect and to decrease response time.

REFERENCES

1]Z. Wu, Z. Chen, X. Du, J. M. Logan, J. Sippel, M. Nikolou, K. Kamaras, J. R. Reynolds, D. B. Tanner, A. F. Hebard, and A. G. Rinzler, Science **305**, 1273 (2004).
2]E. S. Snow, J. P. Novak, P. M. Campbell, and D. Park, Appl. Phys. Lett.**82**, 2145 (2003).
3]P. Bondavalli, P. Legagneux, and D. Pribat, Sens. Actuators B **140**, 304(2009).
4]I. A. Levitsky and W. B. Euler, Appl. Phys. Lett. **83**, 1857 (2003).
5]M. E. Itkis, F. Borondics, A. Yu, and R. C. Haddon, Science **312**, 413(2006).
6]P. Stokes, L. Liu, J. Zou, L. Zhai, Q. Huo, and S. I. Khondaker, Appl. Phys. Lett. **94**, 042110 (2009).
7]B. Pradhan, K. Setyowati, H. Liu, D. H. Waldeck, and J. Chen, Nano Lett.**8**, 1142 (2008).
8]A. E. Aliev, Infrared Phys. Technol. **51**, 541 (2008).
9]M. E. Itkis, S. Niyogi, M. E. Meng, M. A. Hamon, H. Hu, and R. C. Haddon, Nano Lett. **2**, 155 (2002).
10]M. Tarasov, J. Svensson, L. Kuzmin, and E. E. B. Campbell, Appl. Phys. Lett. **90**, 163503 (2007).
11]R. Lu, Z. Li, G. Xu, and J. Z. Wu, Appl. Phys. Lett. **94**, 163110 (2009).
12]A. Fujiwara, Y. Matsuoka, Y. Matsuoka, H. Suematsu, N. Ogawa, K. Miy- ano, H. Kataura, Y. Maniwa, S. Suzuki, and Y. Achiba, Carbon **42**, 919 (2004).
13]A. Yaradanakul, D. P. Butler, and Z. Çelik-Butler, IEEE Trans. Electron Devices **49**, 930 (2002).
14]V. T. S. Wong and W. J. Li, Proceedings of the 2003 IEEE International Symposium on Circuits and Systems, 4, 844 (2003).
15]C. K. M. Fung, V. T. S. Wong, R. H. M. Chan, and W. J. Li, IEEE Trans. Nanotechnol. **3**, 395 (2004).
16]T. W. Ebbesen, H. J. Lezec, H. Hiura, J. W. Bennett, H. F. Ghaemi, and T. Thio, Nature (London) **382**, 54 (1996).
17]S. Selvarasah, C.-L. Chen, S.-H. Chao, P. Makaram, A. Busnaina, and M. R. Dokmeci, Solid-State Sensors, Actuators and Microsystems Confer- ence, 2007, Transducer. International, 1023, (2007).
18]Z. Chen, Z. Wu, L. Tong, H. Pan, and Z. Liu, Anal. Chem. **78**, 8069 (2006).
19]R. Lu, G. Xu, and J. Z. Wu, Appl. Phys. Lett. **93**, 213101 (2008).
20]R. J. Chen, N. R. Franklin, J. Kong, J. Cao, T. W. Tombler, Y. Zhang, and H. Dai, Appl. Phys. Lett. **79**, 2258 (2001).
21]C.-D. Feng, S.-L. Sun, H. Wang, C. U. Segre, and J. R. Stetter, Sens. Actuators B **40**, 217 (1997).
22]S. Maine, C. Koechlin, R. Fleurier, R. Haidar, N. Bardou, C. Dupuis, B. Attal-Trétout, P. Mérel, J. Deschamps, A. Loiseau, and J.-L. Pelouard, Phys. Status Solidi C **7**, 2743 (2010).